AJNR

Assessing Abnormal Iron Content in the Deep Gray Matter of Patients with Multiple Sclerosis versus Healthy Controls

C.A. Habib, M. Liu, N. Bawany, J. Garbern, I. Krumbein, H.-J. Mentzel, J. Reichenbach, C. Magnano, R. Zivadinov and E.M. Haacke

AJNR Am J Neuroradiol 2012, 33 (2) 252-258
doi: https://doi.org/10.3174/ajnr.A2773
http://www.ajnr.org/content/33/2/252

ORIGINAL RESEARCH

Assessing Abnormal Iron Content in the Deep Gray Matter of Patients with Multiple Sclerosis versus Healthy Controls

C.A. Habib
M. Liu
N. Bawany
J. Garbern
I. Krumbein
H.-J. Mentzel
J. Reichenbach
C. Magnano
R. Zivadinov
E.M. Haacke

BACKGROUND AND PURPOSE: It is well known that patients with MS tend to have abnormal iron deposition in and around the MS plaques, in the basal ganglia and the THA. In this study, we used SWI to quantify iron content in patients with MS and healthy volunteers.

MATERIALS AND METHODS: Fifty-two patients with MS were recruited to assess abnormal iron content in their basal ganglia and THA structures. One hundred twenty-two healthy subjects were recruited to establish a baseline of normal iron content in deep GM structures. Each structure was separated into 2 regions: a low-iron-content region and a high-iron-content region. The average phase, the percentage area, and the total phase of the high-iron-content region were evaluated. A weighting was also assigned to each subject depending on the level of iron content and its deviation from the normal range.

RESULTS: A clear separation between iron content in healthy subjects versus patients with MS was seen. For healthy subjects 13% and for patients with MS 65% showed an iron-weighting factor >3 SDs from the normal mean ($P < .05$). The results for those patients younger than 40 years are even more impressive. In these cases, only 1% of healthy subjects and 67% of patients with RRMS showed abnormally high iron content.

CONCLUSIONS: Iron-weighting factors in the basal ganglia, THA, and the midbrain appeared to be abnormal in roughly two-thirds of patients with MS as measured by SWI.

ABBREVIATIONS: CN = caudate nucleus; EDSS = Expanded Disability Status Scale; GM = gray matter; GP = globus pallidus; ICC = intraclass correlation coefficient; PT = pulvinar thalamus; PUT = putamen; RI = normal iron-content region; RII = high iron-content region; RN = red nucleus; RR = relapsing-remitting; SN = substantia nigra; SP = secondary progressive; SPIN = signal processing in nuclear magnetic resonance; THA = thalamus

MS has been considered as both an autoimmune inflammatory demyelinating disease[1] and a disease in which venous involvement is recognized as a possible biomarker or represent some specific damage to the tissue.[2] Recently, the inter-relationship between venous abnormalities, obstructed flow, and a possible role for iron in tissue damage has been considered.[3,4]

To a large degree but not exclusively, the imaging pathogenic landmarks of MS have been well documented mostly in WM.[5,6] To a lesser degree, investigators have noticed abnormalities in cortical regions as well, specifically near the GM/WM boundary and in GM as well.[6,7] However, whether the starting point is in the GM or WM is still unclear.[7-9] Currently, there is an increased interest in studying how GM is affected[6,10,11] and particularly deep GM involvement in MS when iron deposition has been observed.[6,12,13]

Received March 17, 2011; accepted after revision May 24.

From the Departments of Biomedical Engineering (C.A.H., M.L., N.B., E.M.H.), Radiology (C.A.H., M.L., E.M.H.), and Neurology (J.G.), Wayne State University, Detroit, Michigan; Medical Physics Group (I.K., J.R.) and Section of Pediatric Radiology, (H.-J.M.), Institute for Diagnostic and Interventional Radiology I, Center for Radiology, Jena University Hospital, Jena, Germany; Buffalo Neuroimaging Analysis Center (C.M., R.Z.), Jacobs Neurological Institute, University of Buffalo, Buffalo, New York; and The MRI Institute for Biomedical Research (E.M.H.), Detroit, Michigan.

This work was supported by a grant from Siemens Medical Systems.

Please address correspondence to E. Mark Haacke, PhD, MR Research Facility, Department of Radiology, Wayne State University, HUH—MR Research Facility G030/Radiology, 3990 John R Rd, Detroit, MI 48201; e-mail: nmrimaging@aol.com

http://dx.doi.org/10.3174/ajnr.A2773

Brain iron accumulation in neurodegenerative diseases, including MS, is not new and has been shown histologically in the past.[14,15] In MS, its source is likely due to myelin or oligodendrocyte debris, concentrated iron in the macrophages, or as a product of local microhemorrhages following venule wall damage.[6,12] As the wall breaks down, free iron may escape outside the vessel. This process has typically been seen in the basal ganglia, neurons, oligodendrocytes, macrophages, and microglia.[6] Generally, free iron is known to lead to the formation of highly reactive hydroxyl radicals that can trigger cell membrane dysfunction[16] and chronic microglial activation.[1] Thus, iron from any of the above-mentioned sources could lead to inflammation and a further buildup of iron, causing the system to be self-sustainable.[17] When iron is present, the result is a hypointense signal intensity on T2- or T2*-weighted images and a change in the phase for SWI,[9,18,19] which makes it possible to quantify iron changes in vivo. Different results have been reported in studying iron involvement in MS. The variations seen in these results have been related to many factors, including the type of MS studied, the sample size recruited, and the methodologies used to assess iron deposition. A number of studies have now shown that there are increases in iron in the basal ganglia and the THA.[17-19] In a recent study,[19] high iron was found in the PT, the THA, and GP, and the authors considered the iron measured by SWI to be a strong indicator of disability progression, lesion volume accumulation, and atrophy.

Another study by Burgetova et al[20] by using T2 relaxometry

showed that iron does increase in the basal ganglia and the THA of patients with MS, but it showed an inverse correlation with lesion load. Zhang et al[21] also reported a correlation between T2 hypointensities (representing iron deposition) and the patients' disabilities in the RRMS group they studied. Ceccarelli et al[22] investigated deep GM T2 hypointensity in patients with clinically isolated syndrome MS patients and showed that iron-related changes and neurodegeneration can both occur in the early stages of MS. Recent work investigated the potential role that extravasated iron might play by studying CSF ferritin levels, which are considered an indirect measure of iron in the brain.[23] They found no difference between the MS population and the control group. Another study[24] noted that iron deficiency was reported in the MS group studied, and iron supplementation was prescribed to these patients. Evidently, this treatment resulted in a partial recovery of their symptoms. Thus, the role of iron in MS and its correlation with the clinical outcomes are still unclear, and new approaches to investigate brain iron in patients with MS are still needed. In this multidisciplinary work, we study a group of 52 patients with MS by using SWI, which is a powerful MR imaging methodology known to be sensitive to iron. We also present a new weighting scheme to evaluate iron abnormalities and better differentiate between what is considered normal and abnormal iron deposition.

Materials and Methods

Data Acquisition

Fifty-two patients with clinically definite MS were imaged (mean age, 43 ± 11.73 years; range, 17–66 years) under 4 separate internal review board approved protocols. One hundred twenty-two healthy subjects (mean age, 44 ± 13.49 years; range, 20–69 years) were included in this study to establish a normal range of iron deposition in the structures of interest. The patient population studied covered 2 types of MS including patients with RRMS ($n = 31$) and SPMS ($n = 21$) (RRMS mean EDSS score, 2.19; EDSS range, 1–5.5; mean disease duration, 8 years; SPMS mean EDSS score, 5.92; EDSS range, 3–7.5; mean disease duration, 19 years). All patients and controls consented to be subjects in this study. A velocity-compensated 3D gradient-echo sequence was used to generate SWI images.

Site 1. Twelve patients with MS were recruited at the Detroit Medical Center, Detroit, Michigan, for this study. SWI data were acquired on a 1.5T Sonata scanner (Siemens Healthcare, Erlangen, Germany) equipped with an 8-channel head coil. Imaging parameters for SWI were the following: TR = 57 ms, TE = 40 ms, flip angle = 20°, bandwidth = 80 Hz/pixel, FOV = 256 × 192 mm^2, matrix size = 512 × 448, with a resolution of 0.5 × 0.5 × 2 mm^3.

Site 2. Thirty-one patients with MS and 18 healthy subjects were scanned on a 3T Signa Excite HD 12.0 Twin Speed 8-channel scanner (GE Healthcare, Milwaukee, Wisconsin) at the University of Buffalo, Buffalo, New York. A multichannel head and neck coil was used to acquire the SWI data. The imaging parameters were the following: TR = 40 ms, TE = 22 ms, flip angle = 12°, and FOV = 256 × 192 mm^2 (512 × 256 matrix with phase FOV = 0.75) and image resolution of 0.5 × 1× 2 mm^3.

Site 3. Nine patients with MS were scanned by using a 3T TIM Trio system (Siemens Healthcare) at Jena University Hospital, Jena, Germany. A 12-channel receive head-matrix coil was used to acquire the SWI data. The imaging parameters were the following: TR = 29 ms, TE = 20 ms, flip angle = 15°, bandwidth = 120 Hz/pixel, FOV = 256 × 192 mm^2, matrix 512 × 256 with FOV phase = 0.75 corresponding to an image resolution of 0.5 × 1×2 mm^3, integrated parallel acquisition techniques = 2 (24 reference lines), 128 partitions.

Site 4. The SWI data of another 104 healthy subjects (previously studied[25]) were added to the 18 healthy subjects studied at site 2 to create a baseline for iron content in the deep GM nuclei of healthy subjects as a function of age.

The ability to use and compare data from different sites, acquired at different field strengths, lies behind the concept that the phase values will remain constant if the product of field strength to the TE is kept constant and is otherwise independent of field strength or system manufacturer.[26] Thus, no matter what field strength is used, evaluating iron content by using phase images should report consistent results. To experimentally test this concept, we recruited 36 healthy controls from site 1, 2, and 3 who were scanned by using the parameters specific to each site, and we analyzed their data. The results were compared with those of 104 healthy subjects from site 4 and indeed showed that these measured values (from sites 1, 2, and 3) lay within the normal range deduced from site 4 data.

Data Analysis

A 64 × 64 (or equivalent) low-spatial-frequency kernel matrix was used to complex-divide the original *k*-space data to create an effective high-pass-filtered phase image.[26] The resulting SWI filtered-phase images were used as a means to quantify iron content. Seven deep GM structures were studied for iron content (methodology described in previous studies,[18,19,25]) including the following: the GP, the head of the CN, PUT, THA, SN, RN, and PT.

Our in-house software SPIN (MRI Institute for Biomedical Research, Detroit, Michigan) was used for the data analysis. Each structure was separated into 2 regions of interest: RI and RII. Because our interest was to quantify high iron content, our main focus was on RII and the total region (RI + RII). To achieve this quantification, we used the same process described in more detail in Haacke et al.[25] To separate these 2 regions automatically, we based thresholds on the data from recent articles.[27,28] For the structures that were not included in these articles (PT and THA), appropriate thresholds were calculated by analyzing 20 healthy subjects ranging from 20 to 39 years of age. Otherwise, the thresholds were set by using the mean value measured minus 2 times the SD across an elderly population, to be on the conservative side as outlined in Haacke et al[28] and across the above-mentioned 20 healthy subjects. The boundary of each structure was drawn manually by 3 well-trained graduate students, and the high-iron-content region was found automatically by using threshold values. The ICC reliability was evaluated by comparing the results of 5 different subjects from 3 different observers by using the Statistical Package for Social Sciences (SPSS, Chicago, Illinois) software.

All 3 observers evaluated the average iron content of same structure in RII and the normalized area, and the total iron in the PUT. The ICC values for these measures were 0.71, 0.93, and 0.81, respectively. SPIN can output the statistical measures of the total structure and the high-iron-content region for later analysis. We evaluated different measures[19,25]: 1) the fraction of the structure that had high iron content (percentage area), 2) the average putative iron per voxel in RII, and 3) the total putative iron content in the high-iron-content region. The main criterion to differentiate normal from abnormal is that the measured iron content should lie outside the 95% prediction interval lines of the healthy population. Moreover, iron deposition measures were weighted according to their spread around the mean values. This

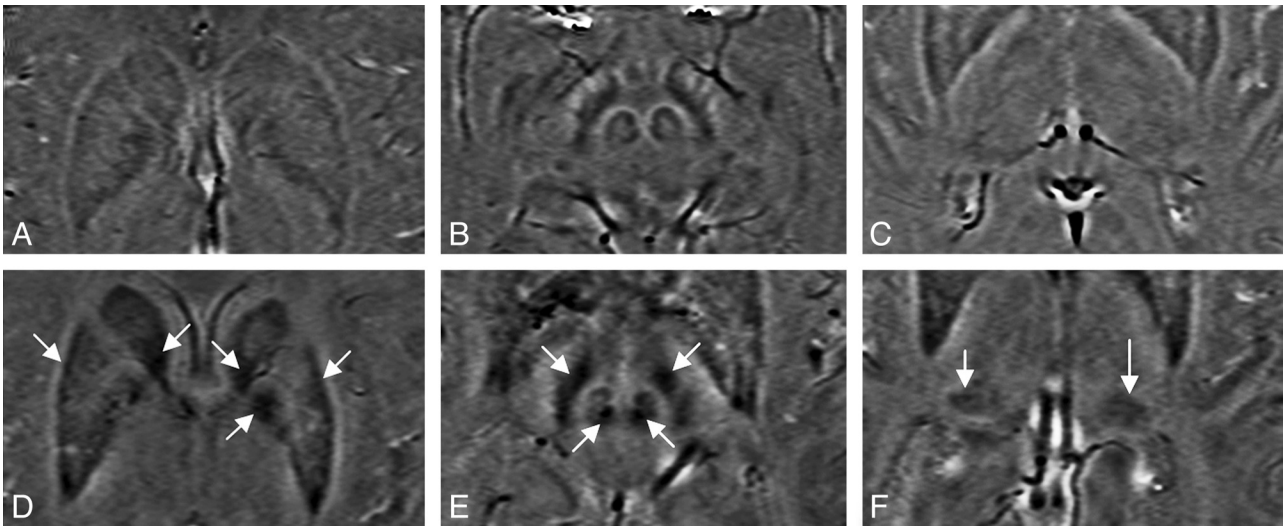

Fig 1. SWI filtered-phase images displaying the basal ganglia and the midbrain of an age-matched healthy control (*A*–*C*) and patient with MS (*D*–*F*), showing abnormal iron deposition in the GP, PUT, and the CN (*D*); the SN and the RN of the midbrain (*E*); and the PT (*F*).

abnormality weighting, AW (m), was achieved by subtracting the measured mean value (MV) from the estimated values of normal iron deposition of age-matched controls, MV_n (calculated from the linear regression), then subtracting m times the estimated SD (SD_n) (m = 2 while considering a 95% confidence interval) and dividing the results by SD_n.

$$AW(m)=[(MV-MV_n)-mSD_n]/SD_n$$

In this article, the results will be shown for both m = 2 and m = 3.

Results

The main purpose of this study was to quantify iron content in the basal ganglia and THA of patients with MS by using phase information acquired from SWI data and to create a new weighting scheme that allows us to better differentiate normal and abnormal iron deposition in patients with MS compared with control subjects. Iron overload was well visualized in patients with MS in a number of regions related to the basal ganglia and THA. Figure 1 displays the iron content visualized in an age-matched control (age, 39 years) and a patient with MS (age, 40 years) in the basal ganglia and midbrain by using SWI. Note that both have iron content in the RN and SN; however, iron overload was only seen in the patient with MS. High iron deposition can be seen in the CN, GP, PUT, and PT of the patient with MS. In the healthy subject, iron deposition in these brain structures is much less and is evenly distributed.

Abnormal iron changes were seen on visual examination in Fig 1, with the quantified results appearing in Fig 2. Generally, the degree of abnormal iron accumulation varied depending on whether one measures total iron in RII, average iron in RII, or the normalized percentage area of RII. In Fig 2, we display these 3 measurements for the CN and PT as an example to show the abnormal iron content of patients with MS relative to healthy subjects.

Figure 3 displays the individual weighting results calculated by using the equation for the PT and RN. A clear separation between healthy subjects and patients with MS was visualized with patients having iron content higher than 3 times the SD of healthy subjects. Figure 4 displays the subtotal weighting of the 4 structures for each measured parameter, including average phase, normalized area, and total phase. The last graph, Fig 4*D*, shows the total weighting of all the parameters of the CN, PT, RN, and SN combined. The figure also demonstrates that there were no healthy controls younger than roughly 40 years of age with abnormal iron content, as reflected by a weight factor of >1.0.

The percentages of individuals with abnormal iron content in both control subjects and patients with MS are shown in Tables 1–3. Note that in these tables, the evaluations and calculations were done for both hemispheres, thereby resulting in a total that is 2 times the number of subjects. In Tables 1 and 2, individual weights (1 parameter for 1 structure), subtotal weights (1 parameter for all the structures), and the total weights (all parameters for all the structures) are displayed for m = 2 and m = 3 (>2 and 3 times the SD, respectively). When we compared healthy subjects with patients with MS ($P < .05$), the total weights showed that 76% of all patients with MS had abnormally high iron content (higher than 2 SDs) in at least 1 of the structures, whereas only 27% of controls had abnormally high iron content. Similar results were seen for subtotal and individual weights (except in the PUT). Results for subjects with iron deposition higher than 3 SDs still show high values for patients with MS.

In Table 3, we display the total and subtotal weights calculated from the CN, PT, RN, and SN iron content that again lie above 2 and 3 times higher than the SD (m = 2 and 3 in the equation). Patients with MS were divided into RR and SP and into 2 age ranges (equal or younger than 40 years and older than 40 years). We found that 27% of the healthy population, 74% of patients with RRMS, and 79% of those with SPMS had iron content above 2 SDs from the mean, while 13% of control subjects had iron content higher than 3 SDs compared with 67% of patients with SPMS and 65% of those with RRMS. The younger RRMS population tended to have a higher percentage of abnormal iron deposition compared with healthy controls for m = 2 and m = 3 except for the subtotal weight–average phase.

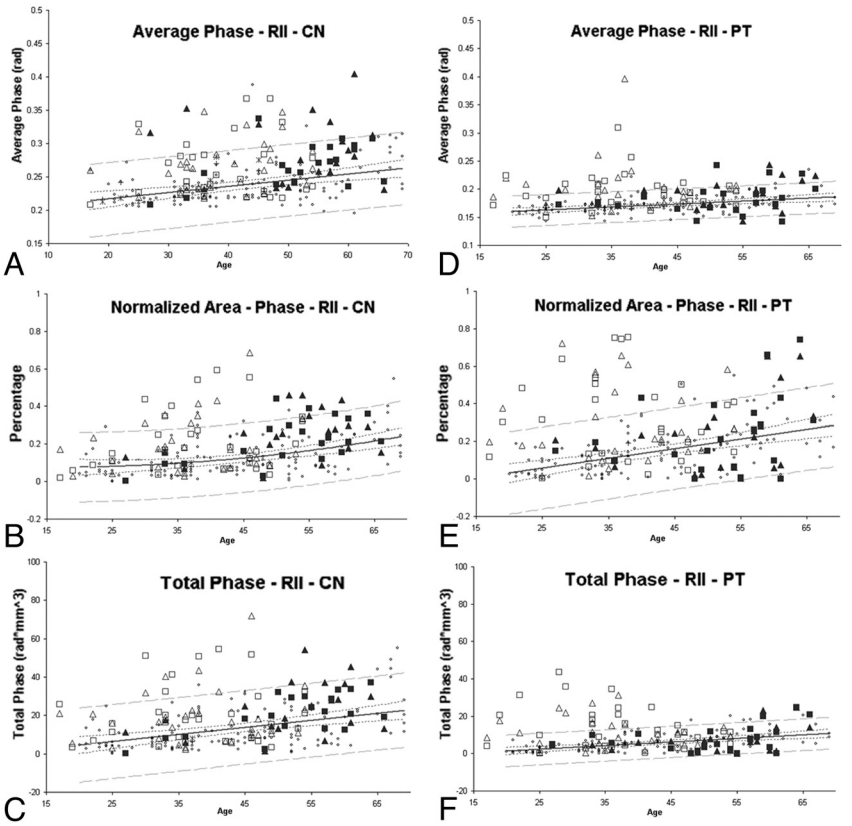

Fig 2. Average phase, normalized area, and total phase of RII in the CN and PT. Small dots represent healthy subjects. The solid line is the regression line, and the outer dashed lines represent the 95% prediction interval of the regression. Hollow squares and triangles represent patients with RRMS, and the solid squares and triangles represent patients with SPMS. The squares and triangles represent the left and right hemispheres respectively. Many of the patients with MS have brain iron content beyond the 95% prediction intervals.

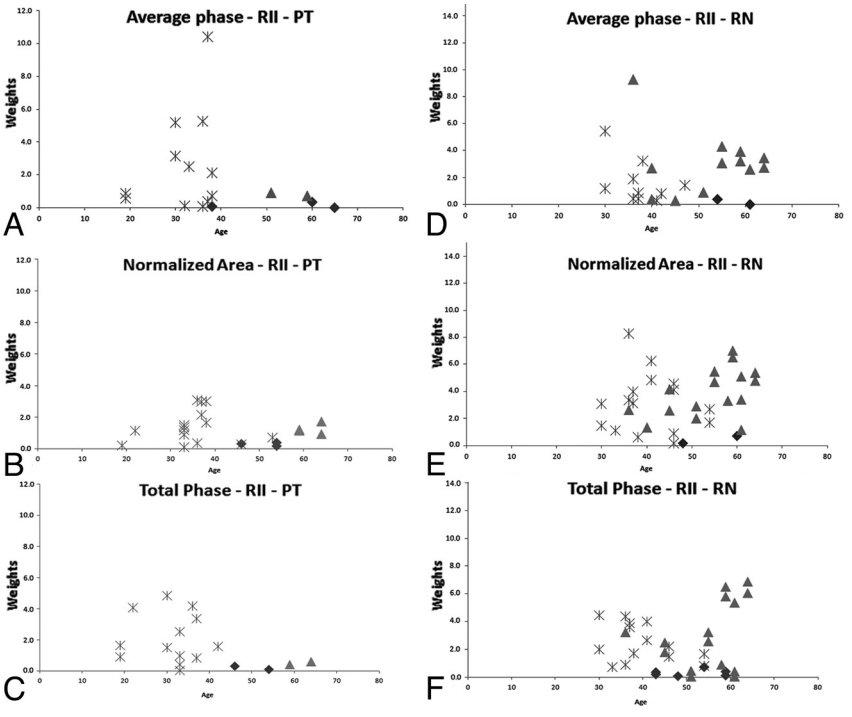

Fig 3. Plots showing individual weighting of different parameters (average phase: upper row; normalized area: middle row; and the total phase: lower row) of the PT (*A*–*C*) and the RN (*D*–*F*). The asterisks represent the patients with RRMS, the triangles represent those with SPMS, and the diamonds represent the healthy subjects. Patients with MS and healthy subjects with weighting higher than 1 are shown in the plots (these results correspond to m = 3; for quantitative evaluation, please refer to Tables 1 and 2).

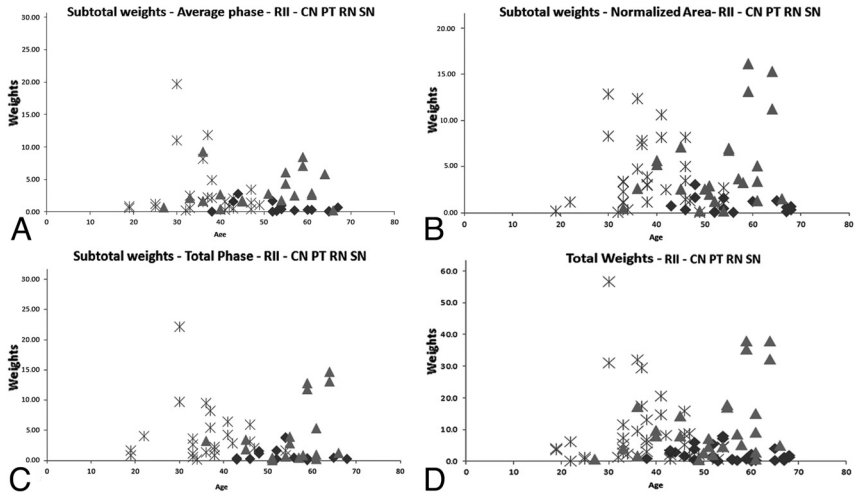

Fig 4. Four plots showing the subtotal (*A*–*C*) weighting factors and the total weighting factor (*D*) of the 4 structures with the weighting factor >1 (these results correspond to m = 3): CN, PT, RN, and SN. The asterisks represent the patients with RRMS, the triangles represent the patients with SPMS, and the diamonds represent healthy subjects. For quantitative results of these graphs, please refer to Table 3.

Table 1: Percentage of healthy and patient subjects with iron deposition higher than 2 SDs (*P* < .05) from the mean based on individual structures

	RII-Average Phase		RII-Normalized Area		RII-Total Phase	
Weights[a]	N	P	N	P	N	P
Subtotal	12.3	62.5	16.4	63.5	16.4	51.9
Individual						
CN	3.7	18.3	4.5	20.2	5.3	12.5
PT	2.0	24.0	4.5	27.9	4.1	23.1
RN	4.5	33.7	6.6	34.6	6.1	30.8
SN	3.7	16.3	4.1	31.7	2.5	22.1
GP	4.5	7.7	3.3	6.7	4.5	5.8
THA	2.9	16.3	3.3	3.8	2.0	3.8
PUT	5.3	3.8	4.1	2.9	5.3	1.0

Note:—N indicates healthy subjects; P, patients.
[a] Total weight for healthy subjects was 27.01, and for patients, 75.81.

Table 2: Percentage of healthy and patient subjects with iron deposition higher than 3 SDs (*P* < .05) from the mean based on individual structures

	RII-Average Phase		RII-Normalized Area		RII-Total Phase	
Weights[a]	N	P	N	P	N	P
Subtotal	5.7	43.3	6.1	52.9	5.7	41.3
Individual						
CN	1.2	14.4	2.0	12.5	0.4	8.7
PT	1.2	13.5	1.2	18.3	0.8	15.4
RN	0.8	21.2	0.8	30.8	2.9	27.9
SN	2.0	10.6	2.0	21.2	2.5	10.6
GP	2.0	4.8	0.8	1.0	2.0	1.0
THA	0.8	6.7	0.0	1.0	0.8	0.0
PUT	2.0	0.0	3.3	1.0	2.5	1.0

Note:—N indicates healthy subjects; P, patients.
[a] Total weight for healthy subjects was 12.7, and for patients, 65.4.

Discussion

The interest in and association of MS with veins and iron deposition are not new.[29] We know that the basal ganglia from the dentate nucleus, the midbrain, and up to the thalamostriate system are all drained by the medial venous drainage system out into the straight sinus. It is just these regions that have increased iron content as seen with SWI and with conventional MR imaging.[4,9] The recent work of Haacke et al[18] suggests that the iron increase seen in MR imaging occurs at the confluence of the small draining veins out of the structures of interest such as the PUT, GP, and CN. Given the previous evidence that MS is a perivenular disease and that iron builds up in the venule wall,[12,30] it may be that these increases in iron represent venous endothelial damage. However, it is still unknown whether iron deposition is a cause or a consequence of the inflammatory demyelinating aspect in MS pathology. On the other hand, the work by Neema et al[9] showed the presence of deep GM T2 hypointensities and suggested that excessive iron deposition is associated with the progression of disease. The plots in Fig 3 show that SPMS and RRMS are well-separated with a dominance of RRMS for younger ages and a dominance of SPMS for older ages.

MR phase information has become more frequently used to evaluate iron content as a function of age in the human brain.[31,32] In previous articles, we introduced the concept of a high-iron content region and normal-iron-content region.[18,25] This made it possible to study not only smaller increases in iron content more confidently but also to study both the average iron content per pixel and the normalized area of increased iron content with age, which showed different and interesting results as mentioned earlier.[19,25] This approach revealed subtle changes in iron content that cannot be seen with the single-region approach because even large increases in iron in a small area would be washed out when looking at iron over the whole region. The variability shown in our results demonstrates that evaluating abnormal iron content is not best achieved by using total iron content measurements. Rather, more information can be obtained by evaluating the area of the high-iron-content region (RII) as well as its average iron content per pixel. These 2 measures appear to present better quantitative indicators of iron content abnormality. In this study, the CN, PT, RN, and SN are shown to be more susceptible to abnormal iron deposition than the other structures studied (with RN being the most susceptible [30%] followed by the PT [27.9%], see Tables 1 and 2). However, no

Table 3: Percentage of healthy and patient subjects with iron deposition higher than 2 and 3 SDs from the mean based on subtotal and total weights[a,b]

	2 SDs			3 SDs		
	RR	SP	Healthy	RR	SP	Healthy
Weights	MS/TMS	MS/TMS	High/Total	MS/TMS	MS/TMS	High/Total
Total						
20–40	28/36 (78%)	6/8 (75%)	15/112 (13%)	24/36 (67%)	4/8 (50%)	1/112 (1%)
41–70	18/26 (69%)	27/34 (79%)	51/132 (38%)	16/26 (62%)	24/34 (71%)	30/132 (23%)
20–70	46/62 (74%)	33/42 (79%)	66/244[b] (27%)	40/62 (65%)	28/42 (67%)	31/244[b] (13%)
Subtotal-normalized area						
20–40	23/36 (64%)	4/8 (50%)	6/112 (5.4%)	19/36 (53%)	4/8 (50%)	0/112 (0%)
41–70	16/26 (62%)	23/34 (68%)	34/132 (26%)	12/26 (46%)	20/34 (59%)	15/132 (11%)
20–70	39/62 (63%)	27/42 (64%)	40/244 (16%)	31/62 (50%)	24/42 (57%)	15/244 (6%)
Subtotal-average phase						
20–40	21/36 (58%)	6/8 (75%)	6/112 (5.4%)	16/36 (44%)	6/8 (75%)	1/112 (1%)
41–70	13/26 (50%)	25/34 (74%)	24/132 (18%)	9/36 (35%)	14/34 (41%)	13/132 (10%)
20–70	34/62 (55%)	31/42 (74%)	30/244 (12%)	25/62 (40%)	20/42 (50%)	14/244 (6%)
Subtotal-total phase						
20–40	21/36 (58%)	4/8 (50%)	5/112 (4.5%)	17/36 (47%)	1/8 (13%)	0/112 (0%)
41–70	10/26 (38%)	19/34 (56%)	35/132 (34%)	8/26 (31%)	17/34 (50%)	14/132 (11%)
20–70	31/62 (50%)	23/42 (55%)	40/244 (16%)	25/62 (40%)	18/42 (43%)	14/244 (6%)

Note:—TMS indicates total number of patients with MS.
[a] Total weights summed over the 4 structures (CN, PT, RN, and SN) and all parameters (average phase, normalized area, and total phase). Subtotal weights summed over the 4 structures (CN, PT, RN, and SN) for individual parameters.
[b] Both the left and right hemisphere measurements were included in this calculation. Since the total number of normal controls is 122, including the left and right measurements together will lead to 244 as the total count. This doubling also applies to the MS population studied. There are 62 values quoted for RR and 42 values for SP, yielding a total of 104.

significant correlation of iron content with EDSS was found with any of the measures we obtained, regardless of the structure studied. This high iron content seen in the basal ganglia, the THA, and the midbrain structures may be consistent with the hypothesis of venous hypertension.[4]

Conclusions

Abnormal iron content by using the total iron-weighting scheme described herein was clearly identified in patients with RRMS, especially those younger than 40 years of age, with almost no abnormal iron seen in the healthy population. Evidently, iron in the basal ganglia, CN, PT, and the midbrain (RN and SN) may be a biomarker for MS. Further work in this direction would be to compare iron content with the severity of venous disease in chronic cerebrospinal venous insufficiency.[4,33]

Disclosures: James Garbern—*Speaker Bureau*: Genzyme, Lundbeck, Details: I am on the speakers' bureau for neurologic conditions other than MS (lysosomal storage disease-Genzyme; Huntington disease-Lundbeck); *Consultant*: EMD-Serono, Biogen, Details: I have done consulting for both companies regarding pharmaceuticals for treatment of MS; *Other Financial Relationships*: PMD Foundation, European Leukodystrophy Association, Details: I have research grants from both of these nonprofit agencies to support my work on Pelizaeus-Merzbacher disease. Robert Zivadinov—*Research Support (including provision of equipment or materials)*: Biogen Idec, Teva Neuroscience, Genzyme, Bracco, Questcor Pharmaceuticals, Greatbatch, EMD-Serono; *Speaker Bureau/Consultant*: Teva Neuroscience, Biogen Idec, EMD Serono, Questcor Pharmaceuticals. E. Mark Haacke—*Research Support (including provision of equipment or materials)*: Siemens, Details: grant for research in SWI.

References

1. Lassmann H, Bruck W, Lucchinetti CF. **The immunopathology of multiple sclerosis: an overview.** *Brain Pathol* 2007;17:210–18
2. Schelling F. **Damaging venous reflux into the skull or spine: relevance to multiple sclerosis.** *Med Hypotheses* 1986;21:141–48
3. Zamboni P, Galeotti R, Menegatti E, et al. **Chronic cerebrospinal venous insufficiency in patients with multiple sclerosis.** *J Neurol Neurosurg Psychiatry* 2009;80:392–99
4. Singh AV, Zamboni P. **Anomalous venous blood flow and iron deposition in multiple sclerosis.** *J Cereb Blood Flow Metab* 2009;29:1867–78. Epub 2009 Sep 2
5. Filippi M, Rocca MA, Martino G, et al. **Magnetization transfer changes in the normal appearing white matter precede the appearance of enhancing lesions in patients with multiple sclerosis.** *Ann Neurol* 1998;43:809–14
6. Haacke EM, Makki M, Ge Y, et al. **Characterizing iron deposition in multiple sclerosis lesions using susceptibility weighted imaging.** *J Magn Reson Imaging* 2009;29:537–44
7. Nelson F, Poonawalla AH, Hou P, et al. **Improved identification of intracortical lesions in multiple sclerosis with phase-sensitive inversion recovery in combination with fast double inversion recovery MR imaging.** *AJNR Am J Neuroradiol* 2007;28:1645–49
8. Allen IV, McQuaid S, Mirakhur M, et al. **Pathological abnormalities in the normal-appearing white matter in multiple sclerosis.** *Neurol Sci* 2001;22:141–44
9. Neema M, Arora A, Healy BC, et al. **Deep gray matter involvement on brain MRI scans is associated with clinical progression in multiple sclerosis.** *J Neuroimaging* 2009;19:3–8
10. Filippi M, Rocca MA. **MR imaging of gray matter involvement in multiple sclerosis: implications for understanding disease pathophysiology and monitoring treatment efficacy.** *AJNR Am J Neuroradiol* 2010;31:1171–77. Epub 2009 Dec 31
11. Varga AW, Johnson G, Babb JS, et al. **White matter hemodynamic abnormalities precede sub-cortical gray matter changes in multiple sclerosis.** *J Neurol Sci* 2009;282:28–33
12. Adams CW. **Perivascular iron deposition and other vascular damage in multiple sclerosis.** *J Neurol Neurosurg Psychiatry* 1988;51:260–65
13. Eissa A, Lebel RM, Korzan JR, et al. **Detecting lesions in multiple sclerosis at 4.7 Tesla using phase susceptibility-weighting and T2-weighting.** *J Magn Reson Imaging* 2009;30:737–42
14. Craelius W, Migdal MW, Luessenhop CP, et al. **Iron deposits surrounding multiple sclerosis plaques.** *Arch Pathol Lab Med* 1982;106:397–99
15. Levine SM, Chakrabarty A. **The role of iron in the pathogenesis of experimental allergic encephalomyelitis and multiple sclerosis.** *Ann N Y Acad Sci* 2004;1012:252–66
16. Gutteridge JM. **Iron and oxygen radicals in brain.** *Ann Neurol* 1992;32(suppl):S16–21
17. Hammond KE, Metcalf M, Carvajal L, et al. **Quantitative in vivo magnetic resonance imaging of multiple sclerosis at 7 Tesla with sensitivity to iron.** *Ann Neurol* 2008;64:707–13
18. Haacke EM, Garbern J, Miao Y, et al. **Iron stores and cerebral veins in MS studied by susceptibility weighted imaging.** *Int Angiol* 2010;29:149–57
19. Zivadinov R, Schirda C, Dwyer MG, et al. **Chronic cerebrospinal venous insufficiency and iron deposition on susceptibility-weighted imaging in patients with multiple sclerosis: a pilot case-control study.** *Int Angiol* 2010;29:158–75
20. Burgetova A, Seidl Z, Krasensky J, et al. **Multiple sclerosis and the accumulation of iron in the basal ganglia: quantitative assessment of brain iron using MRI T(2) relaxometry.** *Eur Neurol* 2010;63:136–43
21. Zhang Y, Metz LM, Yong VW, et al. **3T deep gray matter T2 hypointensity**

correlates with disability over time in stable relapsing-remitting multiple sclerosis: a 3-year pilot study. *J Neurol Sci* 2010;297:76–81
22. Ceccarelli A, Rocca MA, Neema M, et al. **Deep gray matter T2 hypointensity is present in patients with clinically isolated syndromes suggestive of multiple sclerosis.** *Mult Scler* 2010;16:39–44
23. Worthington V, Killestein J, Eikelenboom MJ, et al. **Normal CSF ferritin levels in MS suggest against etiologic role of chronic venous insufficiency.** *Neurology* 2010;75:1617–22
24. van Toorn R, Schoeman JF, Solomons R, et al. **Iron status in children with recurrent episodes of tumefactive cerebral demyelination.** *J Child Neurol* 2010;25:1401–07
25. Haacke EM, Miao YW, Liu M, et al. **Correlation of putative iron content as represented by changes in R2* and phase with age in deep gray matter of healthy adults.** *J Magn Reson Imaging* 2010;32:561–76
26. Haacke EM, Mittal S, Wu Z, et al. **Susceptibility-weighted imaging: technical aspects and clinical applications, part 1.** *AJNR Am J Neuroradiol* 2009;30:19–30
27. Miao Y, Liu T, Wu JL. **Correlation study of susceptibility weighted imaging (SWI) study on deep brain gray nuclei and age.** In*: Proceeding of the 94th Scientific Assembly and Annual Meeting of the Radiological Society of North America,* Chicago, Illinois. November 30-December 5, 2008
28. Haacke EM, Ayaz M, Khan A, et al. **Establishing a baseline phase behavior in magnetic resonance imaging to determine normal vs. abnormal iron content in the brain.** *J Magn Reson Imaging* 2007;26:256–64
29. Haacke EM. **Chronic cerebral spinal venous insufficiency in multiple sclerosis.** *Expert Rev Neurother* 2011;11:5–9
30. Zamboni P. **The big idea: iron-dependent inflammation in venous disease and proposed parallels in multiple sclerosis.** *J R Soc Med* 2006;99:589–93
31. Ogg RJ, Langston JW, Haacke EM, et al. **The correlation between phase shifts in gradient-echo MR images and regional brain iron concentration.** *Magn Reson Imaging* 1999;17:1141–48
32. Xu X, Wang Q, Zhang M. **Age, gender, and hemispheric differences in iron deposition in the human brain: an in vivo MRI study.** *Neuroimage* 2008;40:35–42
33. Zivadinov R, Brown MH, Schirda CV, et al. **Abnormal subcortical deep-gray matter susceptibility-weighted imaging filtered phase measurements in patients with multiple sclerosis. A case-control study.** *Neuroimage* 2012;59:331–9.